UNIVERSITY
OF TRENTO

DIPARTIMENTO DI INGEGNERIA E SCIENZA DELL'INFORMAZIONE

38123 Povo – Trento (Italy), Via Sommarive 14
http://www.disi.unitn.it

AN EXCITATIONMATCHING PROCEDURE FOR SUB-ARRAYED
MONOPULSE ARRAYS WITH MAXIMUM DIRECTIVITY

L. Manica, P. Rocca, and A. Massa

February 2009

Technical Report # DISI-11-038

An Excitation Matching Procedure for Sub-arrayed Monopulse Arrays with Maximum Directivity

L. Manica, P. Rocca, and A. Massa

ELEDIA Research Group

Department of Information and Communication Technology,

University of Trento, Via Sommarive 14, 38050 Trento - Italy

Tel. +39 0461 882057, Fax +39 0461 882093

E-mail: *andrea.massa@ing.unitn.it,*

       {*luca.manica*, *paolo.rocca*}*@dit.unitn.it*

Web-site: *http://www.eledia.ing.unitn.it*

An Excitation Matching Procedure for Sub-arrayed Monopulse Arrays with Maximum Directivity

L. Manica, P. Rocca, and A. Massa

Abstract

In this paper, the maximization of the directivity of compromise difference patterns in sub-arrayed monopulse linear array antennas with optimum sum mode is addressed by means of a two-stage excitation matching procedure. The knowledge of the independently optimum difference excitations, which provide the maximum directivity, is exploited with an efficient matching technique based on the contiguous partition method. Simple and reliable compromise solutions, characterized by a reduced complexity as well as easier antenna manufacturing, are synthesized to assess the effectiveness of the proposed method also in comparison with state-of-the-art methods devoted to the directivity maximization.

1 Introduction

Monopulse tracking systems require antennas that generate at least two different patterns, namely the sum beam and the difference one. Towards this end, different solutions might be taken into account depending on the trade-off among the requirements on optimum sum and difference modes, since some constraints are incommensurable [1] [e.g., reduced circuital complexity, low sidelobe levels ($SLLs$), high directivity, low costs]. In the last years, array antennas have been usually used since they are easy to built and the lobes of the generated patterns can be electronically steered, thus avoiding the use of mechanical systems of positioning.

As far as the feeding network is concerned, compromise solutions are generally adopted because of the limited available space [2]. For such a reason, sub-arraying techniques have been introduced [3]. Sub-arraying strategies are aimed at satisfying one or more user-defined constraint/s on some pattern features with a reduced complexity and a simplification of the antenna manufacturing and assembly with respect to the two-module feed architecture, which provides independent excitations for the sum and difference modes of operation. In the literature, different approaches have been proposed to properly address the problem of synthesizing the optimal compromise between sum and difference patterns to obtain an optimum sum mode and a "*best compromise*" difference one. They consider optimization techniques [4]-[8] as well as excitation matching methods [3][9]. Although optimization techniques can be simply adapt to optimize one or more (at the price of higher computational complexity) pattern features, the major part of the contributions have taken into account the minimization of the SLL [4]-[6][8]. Only in [7], the approach previously presented in [6] was extended to maximize the directivity of the compromise pattern. Within this framework, the Contiguous Partition Method (CPM) [9] has shown its effectiveness and versatility in determining a "*best compromise*" difference pattern close as much as possible to the optimum in the Dolph-Chebyshev sense [10] (i.e., narrowest first null beamwidth and largest normalized difference slope on the boresight for a specified sidelobe level) [9] as well as the optimization of some pattern features (e.g., SLL [11]). In order to further assess the reliability and to point out the flexibility of the CPM, the approach is now extended to the optimization of the directivity of the compromise difference pattern as in [7].

The paper is organized as follows. A brief description of the mathematical formulation of the CPM as well as of its customization to the maximization of the directivity is outlined in Sect. 2. For comparison purposes, some representative results concerned with a set of numerical experiments used in the literature as benchmark test cases are presented and discussed (Sect. 3). Eventually, some conclusions are drawn (Sect. 4).

2 Mathematical Formulation

Let us consider a linear array with $N = 2 \times M$ elements uniformly-spaced (d being the inter-element distance). The sum mode and the difference one are obtained by means of a set of symmetric excitation coefficients $\underline{\Sigma} = \{s_m = s_{-m}; \ m = 1, ..., M\}$ and an anti-symmetric one $\underline{\Delta} = \{d_m = -d_{-m}; \ m = 1, ..., M\}$, respectively.

When sub-arraying techniques [3] are used (Fig. 1), one of the two modes is obtained from the other (optimum) by defining a suitable sub-array configuration and the corresponding weights to satisfy the user-defined requirements. Starting from a fixed and pre-optimized sum mode $\underline{\Sigma}$, the compromise difference pattern $\underline{B}$ is determined as follows

$$\underline{B} = \{b_m = -b_{-m} | \ b_m = s_m \delta_{mq} w_q; \ m = 1, ..., M; \ q = 1, ..., Q\} \tag{1}$$

where w_q ($q = 1, ..., Q$) is the q-th sub-array weight and δ_{mq} is the Kronecker delta function [if $c_m = q$ then $\delta_{mq} = 1$, else $\delta_{mq} = 0$]. Furthermore, $c_m \in [1, Q]$ represent a positive integer value indicating the membership of the m-th element to a sub-array and Q is the number of sub-arrays.

Likewise in [7], the problem at hand is formulated as follows: "*optimizing the sub-array configuration and the corresponding weights in order to synthesize a compromise difference pattern with maximum directivity.*" To properly address such a problem, since (*a*) the CPM is an excitation matching method aimed at reproducing a reference pattern and (*b*) analytical solutions exist to yield a difference pattern with maximum directivity (e.g., see [12][13] for continuous line sources and [14]-[16] when dealing with discrete arrays), a two-stage procedure is detailed as follows. Generally speaking, the first stage is devoted to generate, according to the guidelines

4

in [14], the difference excitation set $\underline{\Delta}_{max} = \{\Delta_m = -\Delta_{-m}; \, m = 1, ..., M\}$ that provides the reference pattern $P_{\underline{\Delta}_{max}}(\theta)$ with maximum directivity $D_{max} = max_\theta \{D(\theta)\}$ without sidelobe constraints, being $D(\theta)$ the directivity function given by

$$D(\theta) = 2 \frac{\sum_{m=1}^{M} \sum_{n=1}^{M} \{d_m F_m(\theta) F_n(\theta) d_n\}}{\sum_{m=1}^{M} \sum_{n=1}^{M} \{d_m G_{mn} d_n\}}, \tag{2}$$

where $F_j(\theta) = sin\left[\frac{kd(2j-1)sin\theta}{2}\right]$, $j = m, n$ and $G_{mn} = \frac{sin[(n-m)kd]}{(n-m)kd} - \frac{sin[(n+m-1)kd]}{(n+m-1)kd}$. Successively, the CPM is used to determine the compromise set $\underline{B}$ close as much as possible to the optimal one $\underline{\Delta}_{max}$ in order to synthesize a pattern $P_{\underline{B}}(\theta)$ with highest directivity. In more detail:

- *Stage 1 - **Computation of the Reference Excitations**, $\underline{\Delta}_{max}$*

  As shown in [14], the reference difference set $\underline{\Delta}_{max}$ is the solution of the following set of M equations

  $$\sum_{n=-M}^{M} \{\Delta_n G_{mn}\} = F_m(\theta_{max}), \quad m = 1, ..., M \tag{3}$$

  where θ_{max} is the angular direction of the maximum directivity (i.e., $\theta_{max} = arg\{max_\theta[D(\theta)]\}$). Unfortunately, the direction θ_{max} is not *a-priori* known and it is computed according to an iterative procedure [14], i being the iteration index. Starting from a trial value $\theta = \theta^{(i)}$ ($i = 0$) equal to the angular direction of the maximum directivity in a uniformly-excited array, the excitations are iteratively updated

  $$\sum_{n=-M}^{M} \{d_n^{(i+1)} G_{mn}\} = F_m(\theta^{(i)}), \quad m = 1, ..., M \tag{4}$$

  until the convergence condition holds true:

  $$\frac{\left| I_\theta \theta^{(i-1)} - \sum_{j=1}^{I_\theta} \theta^{(j)} \right|}{\theta^{(i)}} \leq \eta_\theta, \tag{5}$$

  where I_θ and η_θ are a fixed number of iterations and a fixed numerical threshold, respectively. At the end of the iterative process ($i = I$), $\theta_{max} = \theta^{(I)}$ is found as well as the reference excitations $\underline{\Delta}_{max} = \left\{\Delta_m = d_m^{(I)}; \, m = \pm 1, ..., \pm M\right\}$;

5

- *Stage 2 - **Synthesis of the Compromise Pattern with Maximum Directivity***

Once the reference set $\underline{\Delta}_{max}$ has been determined, the compromise difference pattern with maximum directivity is identified by aggregating the array elements according to the guidelines of the CPM [9]. In particular, the following cost function is defined

$$\Psi_{CPM}\left(\underline{C}\right) = \frac{1}{M}\sum_{q=1}^{Q}\sum_{m=1}^{M}\left|s_m\left(\frac{\Delta_m}{s_m} - \delta_{mq}w_q\left(\underline{C}\right)\right)\right|^2 \qquad (6)$$

and successively minimized to only compute the unknown aggregation vector $\underline{C} = \{c_m; \; m = 1, \dots, M\}$ since the sub-array weights are unequivocally determined through the following relationship

$$w_q\left(\underline{C}\right) = \frac{\sum_{m=1}^{M}\left(s_m\right)^2\delta_{mq}\gamma_m}{\sum_{m=1}^{M}\left(s_m\right)^2\delta_{mq}}, \quad q = 1, ..., Q. \qquad (7)$$

where $\gamma_m = \frac{\Delta_m}{s_m}$. The minimization process is carried out by generating a sequence of sub-array configurations $\left\{\underline{C}^{(k)}; \; k = 1, ..., K\right\}$ that converges to the optimal compromise $\underline{C}^{CPM}$. In more detail, starting from a random configuration $\underline{C}^{(0)}$ obtained by sorting the "optimal" gains γ_m, $m = 1, ..., M$ on a line and randomly selecting $Q - 1$ cutting points, the trial solution is updated $[\underline{C}^{(k)} \leftarrow \underline{C}^{(k+1)}]$ just modifying the membership of the "*border elements*[1]" of the previous one, $\underline{C}^{(k)}$ according to the guidelines detailed in [9]. The process is stopped, by setting $\underline{C}^{CPM} = \underline{C}^{(k_{opt})}$, when the convergence condition holds true. Such a condition is defined in terms of a maximum number of iterations K (i.e., $k > K$) or the stationariness of the CPM cost function value (i.e., $\frac{\left|K_\Psi\Psi_{CPM}^{(k-1)} - \sum_{j=1}^{K_\Psi}\Psi_{CPM}^{(j)}\right|}{\Psi_{CPM}^{(k)}} \leq \eta_\Psi$, being K_Ψ and η_Ψ two user-defined control parameters).

3 Numerical Results

In order to show the potentialities and the limitations of the proposed method, a set of illustrative examples are reported and discussed in this Section. Moreover, some comparisons with the

---

[1] The "*border elements*" are identified by the γ_m indexes of the ordered list $\underline{L} = \left\{\gamma_1 = min_m\left(\frac{\Delta_m}{s_m}\right), ..., \gamma_M = max_m\left(\frac{\Delta_m}{s_m}\right)\right\}$ whose adjacent list values γ_{m-1} or/and γ_{m+1} belong to a different sub-array.

solutions obtained by the *Differential Evolution* (DE) optimization technique in [7] will be considered to point out the effectiveness and computational efficiency of the proposed approach. The first test case (*Test Case 1*) deals with a linear array of $N = 20$ elements spaced of $d = \frac{\lambda}{2}$. The sum excitations $\underline{\Sigma}$ have been set to those of the Dolph-Chebyshev pattern with $SLL = -20\,dB$ [17] and, in the first experiment (*Test Case 1 - Experiment 1*), the number of sub-arrays has been set to $Q = 8$. To illustrate the behavior of the two-stage CPM-based approach ($TS - CPM$ in the following), Figure 2 shows the evolution of the descriptive parameters during the first stage (*Computation of the Reference Excitations*, $\underline{\Delta}_{max}$) of the process. As can be observed, the steady behaviors of $D_{max}^{(i)}$ and $\theta_{max}^{(i)}$ verify just after $I = 5$ iterations (Fig. 2) when the reference pattern $[P_{\underline{\Delta}_{max}}(\theta) = P_{\underline{\Delta}^{(I)}}(\theta),\ I = 5]$ shown in Fig. 3 has been synthesized. The corresponding values of the aperture efficiency [18] for the patterns of Fig. 3 are $\epsilon_T^{(0)} = 1.0000$, $\epsilon_T^{(1)} = 0.8676$, and $\epsilon_T^{(I)} = 0.8626$, respectively. By considering the pattern $P_{\underline{\Delta}_{max}}(\theta) = P_{\underline{\Delta}^{(I)}}(\theta)$ and the corresponding excitations ($\underline{\Delta}_{max} = \underline{\Delta}^{(I)}$) as references, the cost function in (6) has been minimized by means of the CPM to determine the compromise solution $\underline{C}^{CPM}$. The behavior of $\Psi_{CPM}^{(k)}$ during the iterative process is shown in Fig. 4 where also the evolution of the maximum value $D_{max}^{(k)}$ of the synthesized directivity is reported. For comparison purposes, the plot of the DE cost function (i.e., $\Psi_{DE}^{(k)} \triangleq D_{max}^{(k)}$) is given, as well. With reference to Fig. 4 and concerning the computational costs, $k_{opt}^{DE} \simeq 820$ iterations are required by the DE-based approach to reach the final solution in Tab. I, while $k_{opt}^{CPM} = 9$ are enough for the CPM ($T_{tot}^{CPM} = 0.58\,sec$, T_{tot} being the total CPU time needed to reach the stopping criterion) to determine the element memberships and sub-array weights (Tab. I). As far as the maximum directivities $D_{max}^{(k_{opt})}$ of the synthesized compromises are concerned, the values obtained with both the DE and the $TS - CPM$ turn out to be very close the one to the other as well as to the asymptotic ideal value $D_{max}^{ideal} = 12.19$.

In order to give a more general overview of the method performance, the number of sub-arrays has been changed from $Q = 1$ up to $Q = 10$ (*Test Case 1 - Experiment 2*), keeping the same problem geometry and setup. The plots of the maximum directivity values $D_{max}^{(k_{opt})}$ of the compromise patterns $P_{\underline{B}^{(k_{opt})}}$ synthesized with the $TS - CPM$ and the DE-based approach are shown and compared with the ideal achievable threshold (i.e., $D_{max}^{ideal} = 12.19$ [14]) in Fig. 5.

As it can be noticed, the $TS-CPM$ always outperforms the results of the DE although the main differences occur in correspondence with a small number of sub-arrays. As a matter of fact, the improvements for $Q \geq 5$ are negligible (i.e., $\xi_D \cong 0.5\%$, being $\xi_D \triangleq \frac{D_{max}^{TS-CPM} - D_{max}^{DE}}{D_{max}^{ideal}}$) since the directivity values of both $TS-CPM$ and DE are very close to D_{max}^{ideal}. On the other hand, when $Q = 2$, the $TS-CPM$ compromise pattern is characterized by a maximum directivity of almost $\xi_D = 19\%$ greater than that of the DE. Such a result points out the efficiency of the CPM-based approach in enabling the synthesis of sub-arrayed patterns with simple feeding networks and limited numbers of sub-arrays. Furthermore, it is worth to note that the values of the compromise excitations $\underline{B}^{CPM}$ asymptotically tend to the optimal distribution $\underline{\Delta}_{max}$. As a matter of fact and unlike [7], it appears that $\underline{B}^{CPM} = \underline{\Delta}_{max}$ when $Q = M = 10$ (Fig. 6) because of the intrinsic nature of the $TS-CPM$ that belongs to the class of "*excitations matching methods*". In order to point out the degree of fitting among reference and actual patterns allowed by the CPM-based technique, let us analyze the behavior of the pattern matching index Θ

$$\Theta = \frac{\int_{-\pi/2}^{\pi/2} \left| P_{\underline{\Delta}_{max}}(\theta) - P_{\underline{B}^{(k_{opt})}}(\theta) \right| d\theta}{\int_{-\pi/2}^{\pi/2} \left| P_{\underline{\Delta}_{max}}(\theta) \right| d\theta} \tag{8}$$

in Fig. 5. As expected, Θ decreases when Q grows and it goes to 0 value when $Q = M$. For a more thoroughly treatment of the synthesis of linear monopulse antennas, let us take into account the mutual coupling (MC) effects for the sum and difference patterns [19]. In particular, the antenna is supposed being made by an array of thin dipoles of length equal to $\lambda/2$. Accordingly, the relative power pattern of the solution obtained by means of the CPM in Fig. 6 as well as the sum pattern effects are shown in Fig. 7. It is worth notice that the degradation of both patterns when MC effects are included is negligible and it increases in the end fire direction.

The second example (*Test Case 2*) is concerned with a $N = 40$ elements array with inter-element spacing equal to $d = 0.7\,\lambda$. As in [7], the excitation coefficients of the sum mode have been chosen to generate a Taylor pattern [20] with $\bar{n} = 6$ and $SLL = -30\,dB$. Figure 8 shows the behavior of the maximum directivity of the synthesized compromise pattern versus the number of sub-arrays, Q (*Test Case 2 - Experiment 1*). The ideal/asymptotic directivity

value is reported, as well (Fig. 8 - continuous red line). Once again, the CPM-based method significantly outperforms the DE when simpler feeding networks are used. As an example, when $Q = 2$, the $TS - CPM$ plot is closer to D_{max}^{ideal} than the DE. In such a situation, the improvement allowed by the $TS - CPM$ is of about $\xi_D = 28\%$.

As far as the computational issues are concerned, let us consider the configuration with $Q = 10$ sub-arrays as a representative situation (*Test Case 2 - Experiment* 2). Figure 9 shows the optimization of the cost function during the iterative process. As it can be noticed, the number of iterations required by the $TS - CPM$ to get the maximum directivity ($k_{opt}^{CPM} = 14$) is smaller than that of the DE ($k_{opt}^{DE} \simeq 1550$). Moreover, the corresponding CPU-time turns out significantly reduced ($T_{tot}^{CPM} = 1.54\,sec$ vs. $T_{tot}^{DE} \simeq 263.5\,sec$ on a $1.5\,GHz$ PC with $512\,MB$ of RAM). Such an event points out the enhanced efficiency of the $TS - CPM$ in sampling the solution space when compared to that of a stochastic evolutionary method. In order to give further insights on the comparison, the compromise pattern distributions [$P_{\underline{B}^{CPM}}(\theta)$ and $P_{\underline{B}^{DE}}(\theta)$] and the reference/optimal one [14] are shown in Fig. 10, whose values of the aperture efficiency are $\epsilon_T^{ref} = 0.8583$, $\epsilon_T^{CPM} = 0.8590$, and $\epsilon_T^{DE} = 0.8601$, respectively. For completeness, the compromise $TS - CPM$ sub-array configuration and the corresponding weights are reported in Tab. II.

4 Conclusions

In this paper, the optimization of the directivity of the difference compromise beam in sub-arrayed monopulse array antennas has been dealt with. By exploiting the knowledge of the reference difference excitations, which provide maximum directivities, a sub-arraying strategy based on the CPM has been used to synthesize monopulse antennas characterized by a reduced complexity. By integrating the procedure aimed at defining the reference difference with highest directivity, the definition of the sub-array configurations and weights has been carried out in an efficient and effective way thanks to a fast sampling of the solution space by considering the presence of *border elements*. The obtained results have proved the effectiveness of the $TS - CPM$ in providing difference patterns with satisfactory directivity values also when few sub-arrays are used. Furthermore, although the CPM is usually aimed at synthesizing a com-

promise pattern close as much as possible to the reference one, the obtained results positively compared with those from customized (to maximize the directivity) state-of-the-art approaches in facing the optimization of the directivity.

Acknowledgments

References

[1] Skolnik, M. I.: 'Radar Handbook' (McGraw-Hill, 1990, 2nd edn.)

[2] McNamara, D. A.: 'Synthesis of sum and difference patterns for two-section monopulse arrays', *IEE Proc. H Microwaves Antennas Propagat.*, 1988, 135, (6), pp. 371-374

[3] McNamara, D. A.: 'Synthesis of sub-arrayed monopulse linear arrays through matching of independently optimum sum and difference excitations', *IEE Proc. H Microwaves Antennas Propagat.*, 1988, 135, (5), pp. 293-296

[4] Ares, F., Rengarajan, S. R., Rodriguez, J. A., and Moreno, E., 'Optimal compromise among sum and difference patterns through sub-arraying', *Proc. IEEE Antennas Propagat. Symp.*, Baltimore, MD, USA, Jul. 1996, pp. 1142-1145

[5] Lopez, P., Rodriguez, J. A., Ares, F., and Moreno, E., 'Subarray weighting for difference patterns of monopulse antennas: joint optimization of subarray configurations and weights', *IEEE Trans. Antennas Propagat.*, 2001, 49, (11), pp. 1606-1608

[6] Caorsi, S., Massa, A., Pastorino, M., and Randazzo, A., 'Optimization of the difference patterns for monopulse antennas by a hybrid real/integer-coded differential evolution method', *IEEE Trans. Antennas Propagat.*, 2005, 53, (1), pp. 372-376

[7] Massa, A., Pastorino, M., and Randazzo, A., 'Optimization of the directivity of a monopulse antenna with a subarray weighting by a hybrid differential evolution method', *IEEE Antennas Wireless Propagat. Lett.,* 2006, 5, (4), pp. 155-158

[8] D'Urso, M., Isernia, T., and Meliado', E. F., 'An effective hybrid approach for the optimal synthesis of monopulse antennas', *IEEE Trans. Antennas Propagat.*, 2007, 55, (4), pp. 1059-1066

[9] Manica, L., Rocca, P., Martini, A., and Massa, A., 'An innovative approach based on a tree-searching algorithm for the optimal matching of independently optimum sum and difference excitations', *IEEE Trans. Antennas Propagat.*, 2008, 56, (1), pp. 58-66

[10] McNamara, D. A., 'Direct synthesis of optimum difference patterns for discrete linear arrays using Zolotarev distribution', *IEE Proc. H Microwaves Antennas Propagat.*, 1993, 140, (6), pp. 445-450

[11] Rocca, P., Manica, L., and Massa, A., 'Synthesis of monopulse antennas through iterative contiguous partition method', *Electron. Lett.*, 2007, 43, (16), pp. 854-856

[12] Bayliss, E. T., 'Design of monopulse antenna difference patterns with low sidelobes', *Bell System Tech. Journal*, 1968, 47, pp. 623-640

[13] Hannan, P. W., 'Maximum gain in monopulse difference mode', *Trans. IRE Antennas Propagat.*, 1961, 9, (3) pp. 314-331

[14] McNamara, D. A., 'Excitations providing maximum directivity for difference arrays of discrete elements', *Electron. Lett.*, 1987, 23, (15), pp. 780-781

[15] McNamara, D. A., 'Quadratic forms for performance indices of symmetrical and antisymmetrical linear arrays', *Electron. Lett.*, 1987, 23, (4), pp. 148-149

[16] Krupitskii, E. I., 'On the maximum directivity of antennas consisting of discrete radiators', *Sov. Phys. - Dokl.*, 1962, 7, pp. 257-259

[17] Dolph, C. L., 'A current distribution for broadside arrays which optimizes the relationship between beam width and sidelobe level', *Proc. IRE*, 1946, 34, (6), pp. 335-348

[18] Mailloux, R. J.: 'Phased Array Antenna Handbook' (Artech House, 2005, 2nd edn.)

[19] Huang, Z., Balanis, C. A., and Birtcher, C. R., 'Mutual coupling compensation in UCAs: simulations and experiment', *IEEE Trans. Antennas Propagat.*, 2006, 54, (11), pp. 3082-3086

[20] Taylor, T. T., 'Design of line-source antennas for narrow beam-width and low side lobes', *Trans. IRE Antennas Propagat.*, 1955, 3, pp. 16-28

FIGURE CAPTIONS

- **Figure 1.** Sketch of the array configuration.

- **Figure 2.** *Test Case 1 ($M = 10$, $d = \lambda/2$, Dolph-Chebyshev sum pattern [17] - $SLL = -20\,dB$). Stage 1 - Computation of the Reference Excitations, $\underline{\Delta}_{max}$.* Evolution of the maximum value of the directivity $D_{max}^{(i)}$ and its angular direction $\theta_{max}^{(i)}$ versus the iteration index, i.

- **Figure 3.** *Test Case 1 ($M = 10$, $d = \lambda/2$, Dolph-Chebyshev sum pattern [17] - $SLL = -20\,dB$). Stage 1 - Computation of the Reference Excitations, $\underline{\Delta}_{max}$.* Directivity patterns $P_{\underline{\Delta}^{(i)}}(\theta)$ synthesized at the iterations $i = 0$, $i = 1$, and $i = I = 5$ $[P_{\underline{\Delta}_{max}}(\theta)]$.

- **Figure 4.** *Test Case 1 ($M = 10$, $d = \lambda/2$, Dolph-Chebyshev sum pattern [17] - $SLL = -20\,dB$) - Experiment 1 ($Q = 8$). Stage 2 - Synthesis of the Compromise Pattern with Maximum Directivity, $P_{\underline{B}^{(k_{opt})}}$.* Behaviors of the cost function value $\Psi^{(k)}$ and of the maximum directivity value $D_{max}^{(k)}$ versus the iteration index k.

- **Figure 5.** *Test Case 1 ($M = 10$, $d = \lambda/2$, Dolph-Chebyshev sum pattern [17] - $SLL = -20\,dB$) - Experiment 2 ($Q = 1, ..., 10$). Stage 2 - Synthesis of the Compromise Pattern with Maximum Directivity, $P_{\underline{B}^{(k_{opt})}}$.* Plot of the values of $D_{max}^{(k)}$ and Θ versus Q for the $TS - CPM$ and the DE approach.

- **Figure 6.** *Test Case 1 ($M = 10$, $d = \lambda/2$, Dolph-Chebyshev sum pattern [17] - $SLL = -20\,dB$) - Experiment 2 ($Q = 10$). Stage 2 - Synthesis of the Compromise Pattern with Maximum Directivity, $P_{\underline{B}^{(k_{opt})}}$.* Optimal excitations [14] and compromise coefficients determined by the $TS - CPM$ and the DE-based approach.

- **Figure 7.** *Test Case 1 ($M = 10$, $d = \lambda/2$, Dolph-Chebyshev sum pattern [17] - $SLL = -20\,dB$) - Experiment 2 ($Q = 10$) - Mutual Coupling.* Relative sum and difference power patterns for an array of $\lambda/2$ dipoles with mutual coupling effects.

- **Figure 8.** *Test Case 2 ($M = 20$, $d = 0.7\,\lambda$, Taylor sum pattern [20] - $SLL = -30\,dB$) - Experiment 1 ($Q = 1, ..., 20$). Stage 2 - Synthesis of the Compromise Pattern with*

Maximum Directivity, $P_{\underline{B}^{(k_{opt})}}$. Plot of the values of $D_{max}^{(k)}$ and Θ versus Q.

- **Figure 9.** *Test Case 2 ($M = 20$, $d = 0.7\,\lambda$, Taylor sum pattern* [20] *- $SLL = -30\,dB$) - Experiment 2 ($Q = 10$). Stage 2 - Synthesis of the Compromise Pattern with Maximum Directivity*, $P_{\underline{B}^{(k_{opt})}}$. Behaviors of the cost function value $\Psi^{(k)}$ and of the maximum directivity value $D_{max}^{(k)}$ versus the iteration index k.

- **Figure 10.** *Test Case 2 ($M = 20$, $d = 0.7\,\lambda$, Taylor sum pattern* [20] *- $SLL = -30\,dB$) - Experiment 2 ($Q = 10$). Stage 2 - Synthesis of the Compromise Pattern with Maximum Directivity*, $P_{\underline{B}^{(k_{opt})}}$. Comparison among the optimal difference directivity pattern $P_{\underline{\Delta}_{max}}$ [14] and the compromise patterns synthesized at the convergence $P_{\underline{B}^{(k_{opt})}}$ by the CPM-based technique and the DE optimization.

TABLE CAPTIONS

- **Table I.** *Test Case 1 ($M = 10$, $d = \lambda/2$, Dolph-Chebyshev sum pattern* [17] *- $SLL = -20\,dB$) - Experiment 1 ($Q = 8$). Stage 2 - Synthesis of the Compromise Pattern with Maximum Directivity*, $P_{\underline{B}^{(k_{opt})}}$. Sub-array configurations $\underline{C}^{(k_{opt})}$ and weight values $\left\{ w_q^{(k_{opt})};\ q = 1, ..., Q \right\}$ determined by the $TS - CPM$ and DE-based approach.

- **Table II.** *Test Case 2 ($M = 20$, $d = 0.7\,\lambda$, Taylor sum pattern* [20] *- $SLL = -30\,dB$) - Experiment 2 ($Q = 10$). Stage 2 - Synthesis of the Compromise Pattern with Maximum Directivity*, $P_{\underline{B}^{(k_{opt})}}$. Sub-array configurations $\underline{C}^{(k_{opt})}$ and weight values $\left\{ w_q^{(k_{opt})};\ q = 1, ..., Q \right\}$ determined by the $TS - CPM$ and DE-based approach.
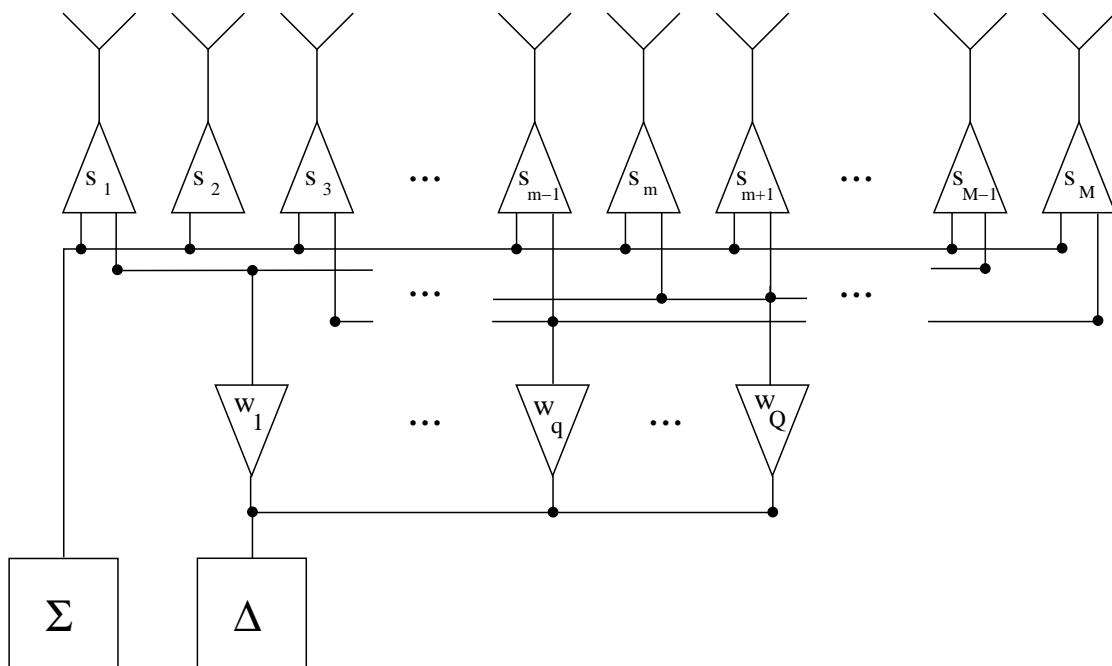
Fig. 1 - L. Manica *et al.,* "An excitation matching procedure for ..."

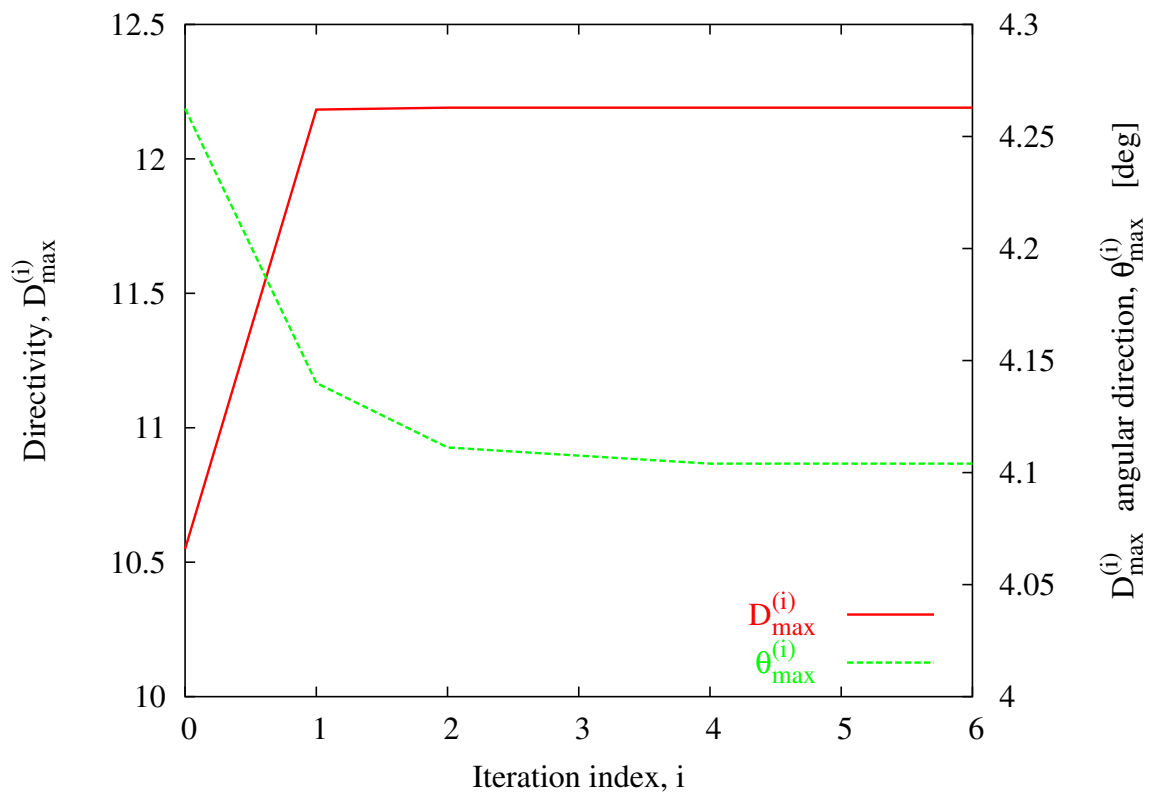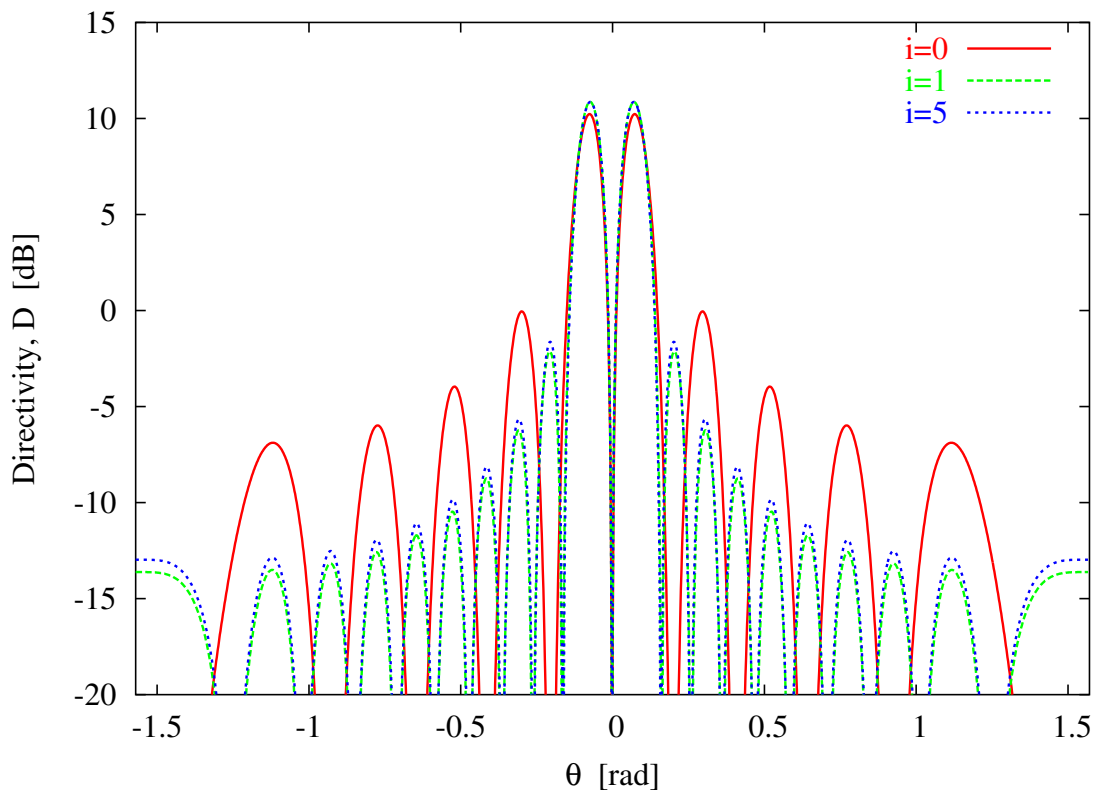**Fig. 2 - L. Manica *et al.,*** "An excitation matching procedure for ..."

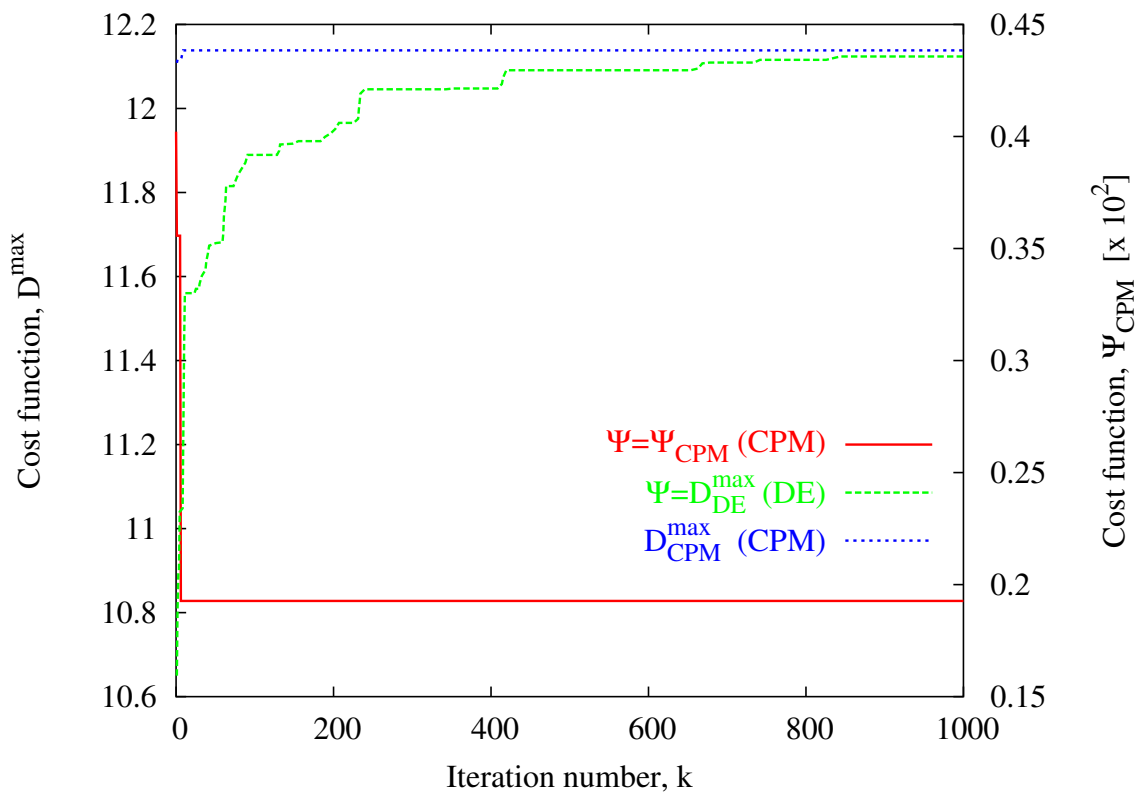**Fig. 3 - L. Manica *et al.,* "An excitation matching procedure for ..."**

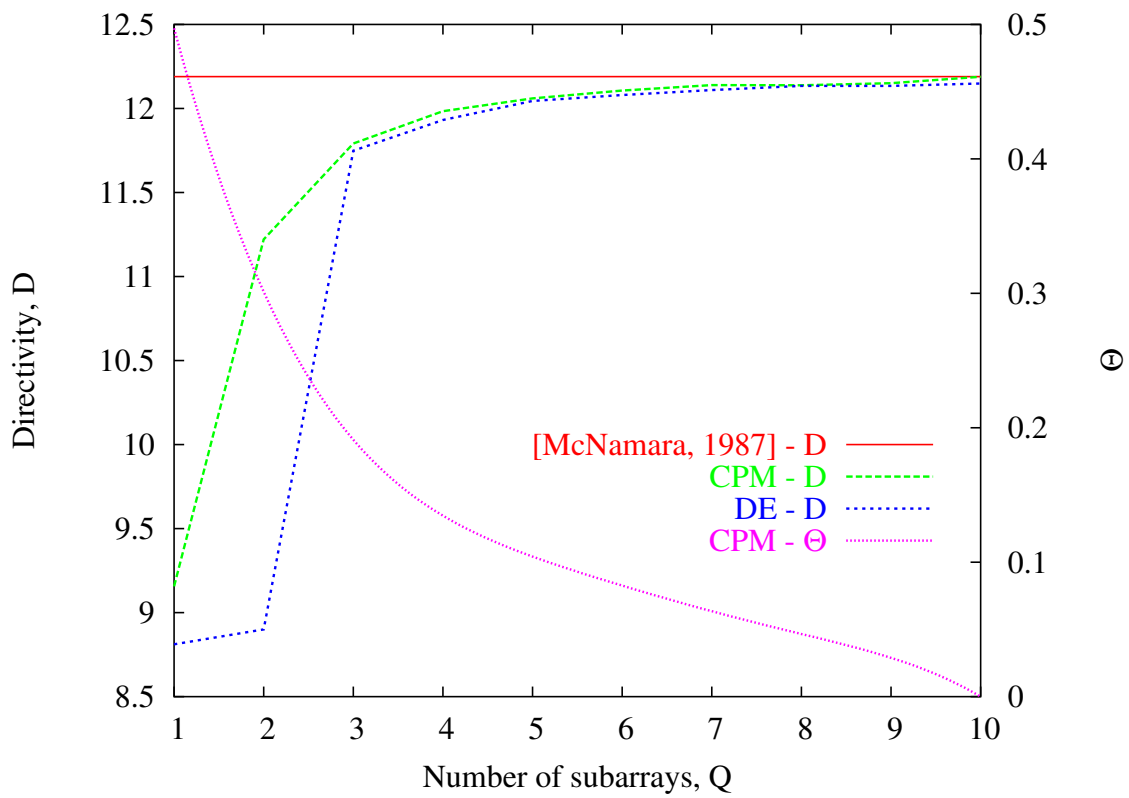**Fig. 4 - L. Manica *et al.,*** "An excitation matching procedure for ..."

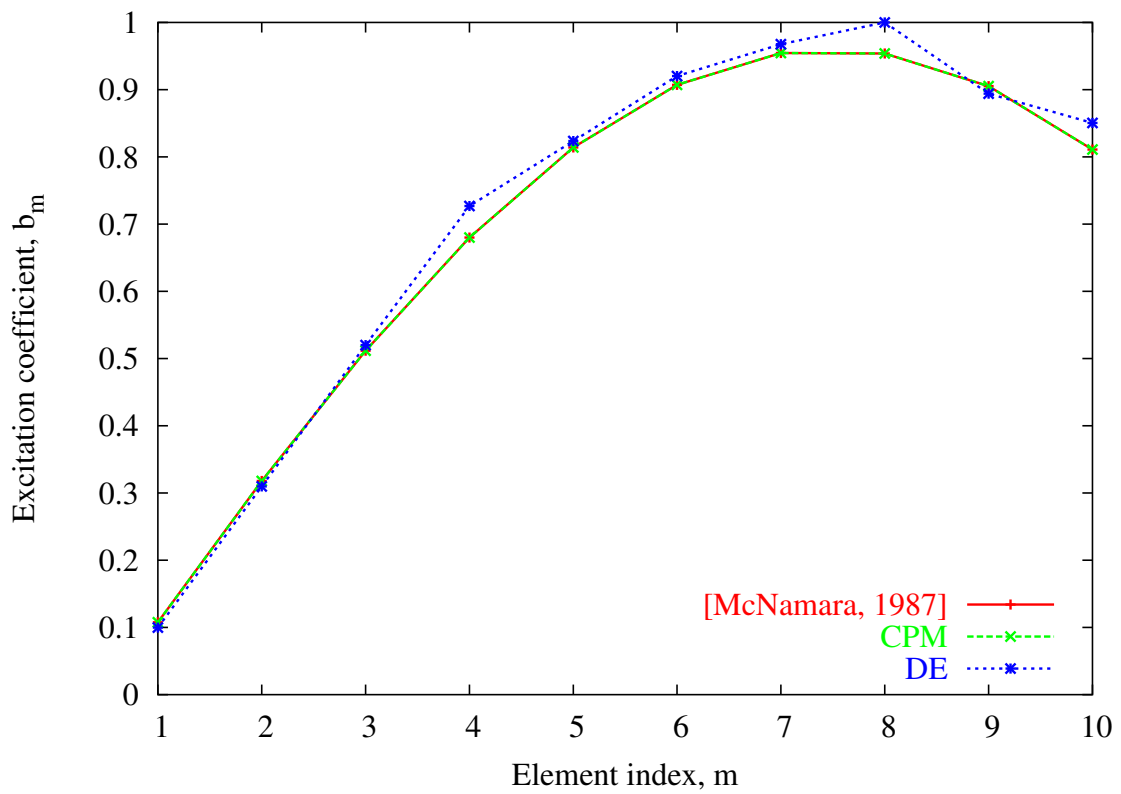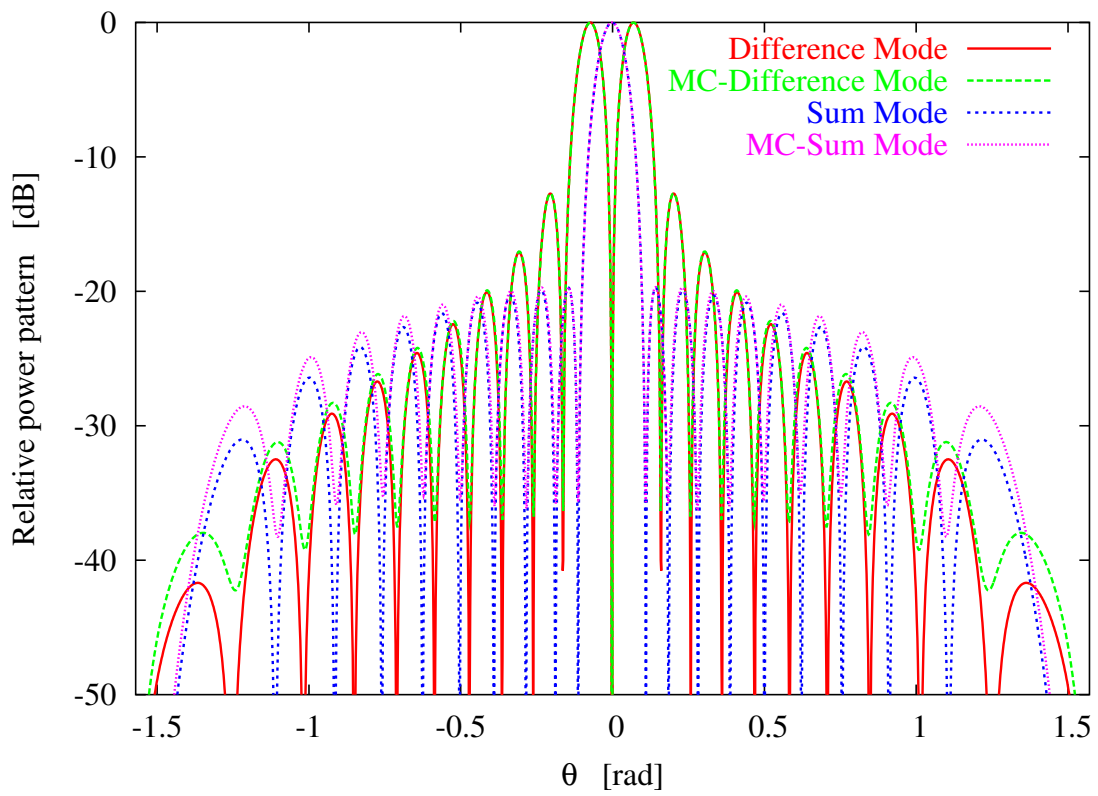**Fig. 5 - L. Manica *et al.,* "An excitation matching procedure for ..."**

Fig. 6 - L. Manica *et al.,* "An excitation matching procedure for ..."

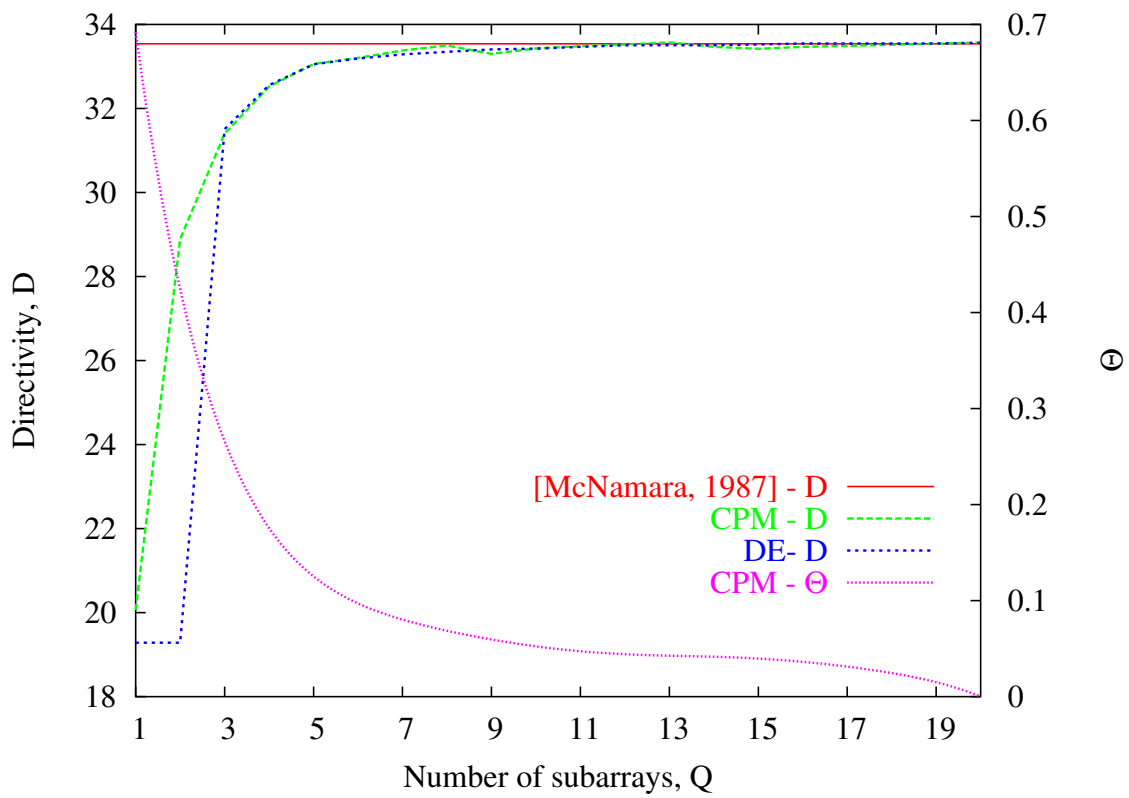**Fig. 7 - L. Manica *et al.,*** "An excitation matching procedure for ..."

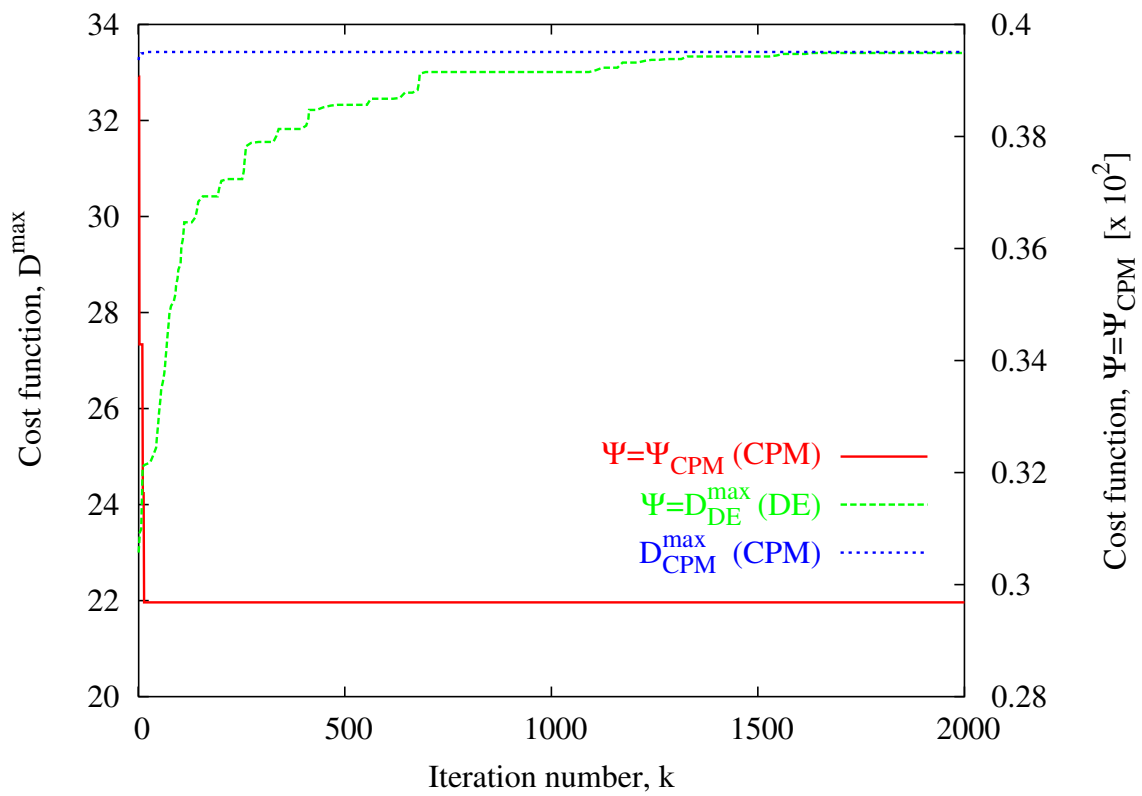**Fig. 8 - L. Manica *et al.,* "An excitation matching procedure for ..."**

Fig. 9 - L. Manica *et al.,* "An excitation matching procedure for ..."

Fig. 10 - L. Manica *et al.,* "An excitation matching procedure for ..."
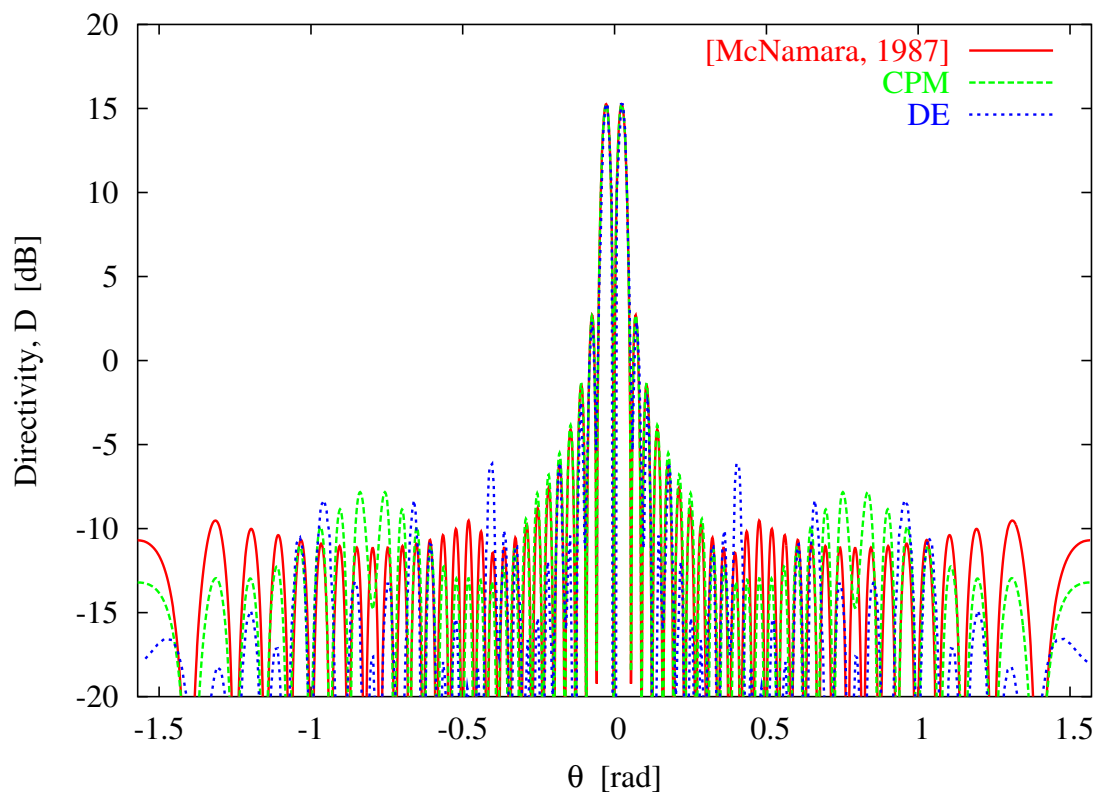
q	1	2	3	4	5	6	7	8
w_q^{CPM}	0.12	0.36	0.60	0.84	1.09	1.34	1.59	1.93
w_q^{DE} [7]	0.12	0.41	0.76	1.11	1.48	1.88	2.38	2.52
$\underline{C}^{CPM}$	1 2 3 4 5 6 7 8 8 4							
$\underline{C}^{DE}$ [7]	1 2 3 4 5 5 6 7 8 4							

Tab. I - L. Manica *et al.,* "An excitation matching procedure for ..."

q	1	2	3	4	5	6	7	8	9	10
w_q^{CPM}	0.109	0.335	0.567	0.842	1.141	1.502	1.994	2.512	2.993	3.316
$\underline{C}^{CPM}$	1 1 2 2 3 3 4 4 5 5 6 6 7 7 8 8 9 10 9 10									

Tab. II - L. Manica *et al.*, "An excitation matching procedure for ..."